A Highly Accurate Feedback Approximation for Horizontal Variable-Speed Interceptions

Hendrikus G. Visser*
Fokker B.V., Amsterdam, the Netherlands
and
Josef Shinar†
Technion—Israel Institute of Technology, Haifa, Israel

An improved feedback approximation of the time-optimal control strategy in a horizontal, variable-speed, air-to-air interception is presented. The improvements are achieved by reformulating the previously used multiple-time scale, forced singular perturbation model and by incorporating first-order correction terms in the control law. Comparison of the uniformly valid feedback approximation with the exact open-loop control solution shows a remarkable payoff accuracy, even for very short initial ranges. Consequently, the domain of validity of the feedback approximation is greatly extended, enhancing its attractiveness as an improved building block in future airborne implementations.

Nomenclature

C_{D_0} = zero-lift drag coefficient
$C_{L_{max}}$ = maximum lift coefficient
D = drag force
D_i = induced drag in straight flight
D_0 = zero-lift drag force
d = capture radius
f = dynamic function (with subscript)
g = acceleration of gravity
H = Hamiltonian
I = integral (with subscript)
J = payoff function
K = induced-drag parameter
L = lift force
n = aerodynamic load factor
n_L = lift-limited load factor
n_{max} = structural load factor limit
q = dynamic pressure
R = separation distance
r = interceptor's turning radius
S = wing area
s = distance in straight flight
T = thrust
t = time
V = interceptor's velocity
V_c = corner velocity
V_T = target velocity
W = interceptor weight
β = difference between line-of-sight angle and interceptor's heading
ϵ = artificial perturbation parameter
ϵ_g = geometric perturbation parameter
η = throttle parameter
Λ = feedback adjoint approximation
λ = adjoint variable (with subscript)
μ = interceptor's bank angle
ρ = air density
τ = stretched time
χ = interceptor's heading
ψ = line-of-sight angle
ω = normalized bank angle

Superscripts

b = boundary layer
i = inner expansion
o = outer expansion
r = reduced-order
s = singular
$\bar{(\ )}$ = previous FSP model (see Refs. 1-3)
$(\ )^*$ = optimal value

Subscripts

f = final value
o = initial value
ss = steady-state value
u = unconstrained value
0 = zeroth-order term
1 = first-order term
0-1 = term corrected to first order

Received July 17, 1985; presented as Paper 85-1783 at the AIAA Atmospheric Flight Mechanics Conference, Snowmass, CO, Aug. 19-21, 1985; revision received April 29, 1986.

*Technical Staff Member, Space Division.
†Professor, Department of Aeronautical Engineering.

Introduction

A ZEROTH-ORDER explicit feedback approximation of the optimal turning strategy for minimum-time, variable-speed, horizontal interception with air-to-air missiles was first presented in Ref. 1. The analysis was carried out by using a multiple-time scale, forced singular perturbation (FSP) model based on the assumption that the line-of-sight rate is very slow compared to aircraft turning dynamics. This model also assumed that the speed variations are slower than the turning dynamics and exhibit a definite time scale separation compared to the changes in relative geometry. The horizontal FSP model became one of the building blocks in subsequent efforts to extend this computational concept to analyze the more realistic three-dimensional interception scenario.[2,3] The main advantage of such a feedback approximation has been its attractiveness for real-time onboard implementation. This potential was validated recently by "pilot-in-the-loop" simulations as well as in actual flight tests.

The accuracy assessment of the FSP approximations started several years ago[2] and is still an ongoing investigation. For the

horizontal case, the comparison to the exact solution indicated that the zeroth-order FSP approximation can provide a reasonable payoff accuracy (less than 1% error in the time of interception) for medium- and long-range engagements in which the maximum speed of the interceptor is nearly reached. Based on these results, the domain of a validity of the zeroth-order FSP approximation is limited to engagements where final speed is not very different from the maximum speed and to initial ranges larger than 8–10 turning radii (minimum radius at the initial speed) of the interceptor.

The origin of these limitations is the imperfect time scale separation between the variables of the FSP model, namely, 1) the speed dynamics is not fast enough compared to variations of relative geometry and 2) the line-of-sight rate is not negligible compared to the aircraft turning rate.

For these reasons, the previously used multiple-time-scale FSP model has to be re-examined. Moreover, further accuracy improvement can be expected if the FSP approximation is corrected to first (or higher) order. The first attempt in this direction was made in a missile optimization problem.[4] The algorithm that computed the first-order correction terms was based on a predictive integration of the slow variables along the zeroth-order boundary-layer transition trajectory. This step had to be iterated until the matching conditions were satisfied. Such a process, having clearly an off-line character, could not be considered as a part of a true feedback solution. At that time, such a property seemed to be an inherent limitation of the FSP approach,[5] but, fortunately, this pessimistic assertion turned out to be incorrect. Recently, it has been demonstrated[6] that, for a class of singular perturbation problems (which includes the horizontal interception), the optimal feedback control can be constructed in a form of a single uniformly valid power series expansion of the perturbation parameter. The terms of this expansion are computed by recursive solution of the Hamilton-Jacobi-Bellman equation. In another recent paper,[7] the first-order correction terms for constant-speed interception were computed analytically and were expressed in an explicit feedback form based on the approach of matched asymptotic expansions.

In the present paper, the new feedback correction method of Ref. 7 is applied to variable-speed interceptions in the horizontal plane using realistic aerodynamic and propulsion models. The solution is based on reformulation of the FSP model of Ref. 1 by including interception velocity dynamics in the "reduced-order" problem. It is followed by incorporating the analytically computed first-order correction terms in the turning boundary-layer control. Based on this boundary-layer control, a uniformly valid feedback control law is synthesized. The accuracy of the first-order FSP approximation is tested by comparison to the exact open-loop solution of the same optimal control problem, obtained by retrograde integration.

Formulation of the Horizontal Interception

Dynamic Equations

The kinematic equations describing the relative horizontal motion of the two aircraft are expressed in a polar coordinate frame (see Fig. 1) as

$$\dot{R} = V_T \cos\psi - V\cos(\psi-\chi), \qquad R(T_o) = R_o \tag{1}$$

$$\dot{\psi} = [-V_T \sin\psi + V\sin(\psi-\chi)]/R, \qquad \psi(t_o) = \psi_o \tag{2}$$

The target flies a straight-line course with constant speed. A point/mass model is used to represent the dynamics of the interceptor. By assuming that 1) thrust T is directed along the flight path, 2) vehicle weight W is constant, and 3) drag D is expressed by a parabolic form, the dynamic equations of motion can be written as

$$\dot{V} = g[T-D]/W, \qquad V(t_o) = V_o \tag{3}$$

$$\dot{\chi} = g[n\sin\mu]/V, \qquad \chi(t_o) = \chi_o \tag{4}$$

where for a given altitude

$$T = \eta T_{\max}(V) \tag{5}$$

$$D = D_0 + n^2 D_i \tag{6}$$

$$D_0 = C_{D_0}(V) qS \tag{7}$$

$$D_i = K(V) W^2/(qS) \tag{8}$$

$$q \triangleq \tfrac{1}{2}\rho V^2 \tag{9}$$

$$n \triangleq (L/W) \tag{10}$$

The condition of vertical force equilibrium relates the bank angle μ to the load factor n by

$$n = 1/\cos\mu \tag{11}$$

allowing the elimination of either μ or n from the problem formulation.

The interceptor's motion is governed by two independent control variables: the throttle parameter η and the bank angle μ (or alternatively the load factor n), which are subject to the following constraints:

$$0 \le \eta \le 1 \tag{12}$$

$$n \le n_L(V) \triangleq \frac{qS}{W} C_{L_{\max}}(V) \quad \text{if } V < V_C \tag{13}$$

$$n \le n_{\max} \quad \text{if } V \ge V_c \tag{14}$$

where the "corner velocity" is defined by

$$V_c \triangleq \left(\frac{2n_{\max} W}{\rho S C_{L_{\max}}}\right)^{1/2} \tag{15}$$

For convenience, let us define the following:

$$f_R(\psi, V, \chi) \triangleq V_T\cos\psi - V\cos(\psi-\chi) \tag{16}$$

$$f_\psi(R, \psi, V, \chi) \triangleq [-V_T\sin\psi + V\sin(\psi-\chi)]/R \tag{17}$$

$$f_V(V, \mu) \triangleq g[T - D_0 - (1+\tan^2\mu)D_i]/W \tag{18}$$

$$f_\chi(V, \mu) \triangleq g\tan\mu/V \tag{19}$$

Note that Eqs. (16–19) represent the right-hand sides of the dynamic equations (1–4) from which the load factor n is eliminated using Eq. (11).

Optimal Control Formulation

Successful interception (capture) is determined by the condition

$$R(t_f) = R_f = d, \qquad \dot{R}(t_f) < 0 \tag{20}$$

where d is the "capture radius" representing the interceptor's firing envelope.

The objective of the interceptor is to select the controls η^* and μ^*, subject to the constraints of Eqs. (12–14), that transfer the state vector (R, ψ, V, χ) from a given set of initial conditions $(R_o, \psi_o, V_o, \chi_o)$ to the terminal condition of Eq. (20) in minimum time, i.e.,

$$J^* = \min_{\eta,\mu} J = \min_{\eta,\mu} \int_{t_o}^{t_f} dt \tag{21}$$

Necessary Conditions of Optimality

The variational Hamiltonian of the problem is defined as

$$H=-1+\lambda_R f_R+\lambda_\psi f_\psi+\lambda_V f_V+\lambda_\chi f_\chi+\text{constraints} \tag{22}$$

The system of adjoint equations and the set of transversality conditions arise from the necessary conditions for optimality as

$$\dot{\lambda}_R=-\frac{\partial H}{\partial R}=\frac{\lambda_\psi f_\psi}{R} \tag{23}$$

$$\dot{\lambda}_\psi=-\frac{\partial H}{\partial \psi}=-\lambda_R f_\psi R+\frac{\lambda_\psi f_R}{R}, \qquad \lambda_\psi(t_f)=0 \tag{24}$$

$$\dot{\lambda}_V=-\frac{\partial H}{\partial V}=\lambda_R\cos(\psi-\chi)-\frac{\lambda_\psi\sin(\psi-\chi)}{R}$$
$$-\lambda_V\frac{g}{W}\frac{\partial(T-D)}{\partial V}+\lambda_\chi\frac{g}{V^2}\tan\mu$$
$$-\frac{\partial}{\partial V}(\text{constraints}), \quad \lambda_V(t_f)=0 \tag{25}$$

$$\dot{\lambda}_\chi=-\frac{\partial H}{\partial \chi}=\lambda_R V\sin(\psi-\chi)+\frac{\lambda_\psi V\cos(\psi-\chi)}{R}, \qquad \lambda_\chi(t_f)=0 \tag{26}$$

Since the system is autonomous and the final time t_f is not prescribed, one has along the optimal trajectory the first integral

$$H^*=0 \tag{27}$$

The optimal control functions are found by applying the maximum principle

$$\eta^*=\tfrac{1}{2}[1+\text{sign}\lambda_V], \qquad \lambda_V\neq 0 \tag{28}$$

For the present problem, a singular thrust arc with $\lambda_V=\dot{\lambda}_V=0$ is not optimal.

$$\mu^*=\min[\,|\mu_u|,\mu_{n_L},\mu_{n_{\max}}]\,\text{sign}(\lambda_\chi), \qquad \lambda_\chi\neq 0 \tag{29}$$

where μ_u is the unconstrained bank angle given by

$$\tan(\mu_u)=\frac{\lambda_\chi}{\lambda_V}\frac{W}{2D_i} \tag{30}$$

and μ_{n_L} and $\mu_{n_{\max}}$ are the positive bank angle constraints from Eqs. (13) and (14).

The eventual case of $\dot{\lambda}_\chi=\lambda_\chi=0$ is a singular trajectory characterized by

$$\tan(\psi-\chi^s)=-\lambda_\psi/R\lambda_R \tag{31}$$

Fortunately, the system of the relative geometry adjoint Eqs. (23) and (24) can be solved in a closed form[8] by using the transversality conditions and Eq. (27). This solution yields

$$\lambda_R=\frac{\cos(\psi-\psi_f)}{V_T\cos\psi_f-V_f\cos(\psi_f-\chi_f)} \tag{32}$$

$$\lambda_\psi=\frac{-R\sin(\psi-\psi_f)}{V_T\cos\psi_f-V_f\cos(\psi_f-\chi_f)} \tag{33}$$

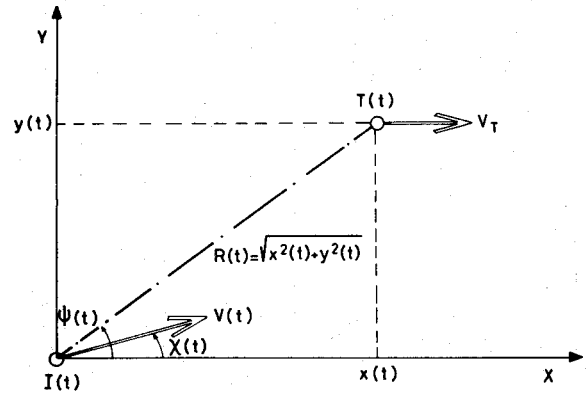

Fig. 1 Geometry of horizontal interception.

Substituting Eqs. (32) and (33) into Eq. (31) indicates that the singular trajectory is a straight line given by

$$\chi^s=\psi_f \tag{34}$$

and consequently

$$\mu^s=0 \tag{35}$$

Open-Loop Solution

The numerical solution of the above formulated optimal control problem leads to a nonlinear two-point boundary value problem consisting of Eqs. (1-4) and (23-26) by substituting the optimal control expressions of Eqs. (28-30). The first integral [Eq. (27)] is redundant and can replace any of the adjoint equations.

In the present paper, the exact numerical solution of the optimal control is needed for the sake of comparison. Such a solution can be also obtained by retrograde integration of the state and costate equations starting at the terminal condition of Eq. (20) and with assumed values of the other "free" final-state variables (ψ_f, V_f, χ_f). By varying these parameters, the state-space can be filled with extremals. An iterative search for an extremal trajectory that passes through a given initial state requires a substantial amount of computation. However, the above outlined approach is suitable for generating an exact solution to be used as a basis for a quantitative comparison. For this purpose, any point on the extremal can be accepted as an initial condition and no iteration process is required. In the present paper, the exact optimal solution is generated by this approach for an arbitrarily selected terminal state and will be compared to the various feedback approximations.

Zeroth-Order Forced Singular Perturbation Analysis

Previous FSP Model[1]

In order to find a feedback approximation to the optimal control solution of the above formulated minimum-time air-to-air interception in the horizontal plane, the following multiple-time scale, forced singular perturbation model was used[1]

$$\dot{R}=f_R(\psi,V,\chi), \qquad R(t_o)=R_o, \qquad R(t_f)=d \tag{36}$$

$$\dot{\psi}=f_\psi(R,\psi,V,\chi), \qquad \psi(t_o)=\psi_o \tag{37}$$

$$\epsilon\dot{V}=f_V(V,\mu), \qquad V(t_o)=V_o \tag{38}$$

$$\epsilon^2\dot{\chi}=f_\chi(V,\mu), \qquad \chi(t_o)=\chi_o \tag{39}$$

where f_R, f_ψ, f_V, and f_χ are determined by Eqs. (16-19).

The methodology of zeroth-order FSP analysis has been explained in detail in several previous publications[1-5,9,10] and, therefore, will not be repeated here. For the sake of conciseness only, the main results of Ref. 1 are recalled. The

variables of this previous zeroth-order feedback approximation are denoted by an overbar (¯).

The reduced-order solution obtained by setting $\epsilon=0$, (denoted by superscript r) was a straight-line trajectory characterized by

$$\bar{V}^r = V_{\max} \triangleq \arg[T_{\max} = D_0 + D_i] \tag{40}$$

$$\bar{\chi}^r = \psi_f = \psi + \Delta\bar{\psi} - \sin^{-1}\left[\frac{V_T \sin(\psi+\Delta\bar{\psi})}{\bar{V}^r}\right] \tag{41}$$

$$\Delta\bar{\psi} = \tan^{-1}\left[\frac{\sin\psi}{(\bar{V}^r R/V_T d) - \cos\psi}\right] \tag{42}$$

$$\bar{\lambda}_R^r = \left[\frac{\cos(\psi-\bar{\chi}^r)}{V_T\cos\chi^{-r} - \bar{V}^r}\right] \tag{43}$$

$$\bar{\lambda}_\psi^r = -\frac{R\sin(\psi-\bar{\chi}^r)}{V_T\cos\bar{\chi}^r - \bar{V}^r} \tag{44}$$

The solution of the outer (velocity) boundary layer yielded

$$\bar{\lambda}_V^r = \frac{W}{g}\frac{(\bar{V}^r - V)}{(\bar{V}^r - V_T\cos\bar{\chi}^r)(T_{\max} - D_0 - D_i)} > 0 \tag{45}$$

and consequently

$$\bar{\eta} = 1 \tag{46}$$

while the inner (turning) boundary-layer solution led [by substituting Eqs. (40-45) into Eqs. (27) and (30)] to a uniformly valid feedback expression for the unconstrained bank angle

$$\tan(\bar{\mu}_u) = \frac{V}{g}\dot{\chi}_{ss}\left(\frac{2V}{\bar{V}^r - V}\right)^{1/2}\sin\left(\frac{\bar{\chi}^r - \chi}{2}\right) \tag{47}$$

relating it to the steady state during rate $\dot{\chi}_{ss}$, defined by

$$\dot{\chi}_{ss} \triangleq \frac{g}{V}\left(\frac{T_{\max} - D_0}{D_i} - 1\right)^{1/2} = \dot{\chi}_{ss}(V) \tag{48}$$

This zeroth-order approximation was found to be reasonably accurate if during the interception the maximum velocity $\bar{V}_r$ is reached. Otherwise, the transversality condition of Eq. (25) is violated. This violation, which frequently occurs in medium-range interceptions, indicates that the assumed time-scale separation between the velocity V and the relative geometry R, ψ is not adequate and may result in a substantial error.

Modified FSP Model

In order to avoid such difficulty, sound engineering judgment suggests that one should analyze all three variables (R,ψ,V) on the same time scale. Therefore, in the forthcoming analysis, the following FSP model will be used:

$$\dot{R} = f_R(\psi,V,\chi), \quad R(t_o) = R_o, \quad R(t_f) = d \tag{49}$$

$$\dot{\psi} = f_\psi(R,\psi,V,\chi), \qquad \psi(t_o) = \psi_o \tag{50}$$

$$\dot{V} = f_V(V,\mu), \qquad V(t_o) = V_o \tag{51}$$

$$\epsilon\dot{\chi} = f_\chi(V,\mu), \qquad \chi(t_o) = \chi_o \tag{52}$$

The corresponding equations and transversality conditions are written as

$$\dot{\lambda}_R = -\frac{\partial H}{\partial R} \tag{53}$$

$$\dot{\lambda}_\psi = -\frac{\partial H}{\partial \psi}, \qquad \lambda_\psi(t_f) = 0 \tag{54}$$

$$\dot{\lambda}_V = -\frac{\partial H}{\partial V}, \qquad \lambda_V(t_f) = 0 \tag{55}$$

$$\epsilon\dot{\lambda}_\chi = -\frac{\partial H}{\partial \chi}, \qquad \lambda_\chi(t_f) = 0 \tag{56}$$

where H remains the same as defined in Eq. (22).

The optimal control conditions given by Eqs. (28-30), as well as the first integral condition [Eq. (27)], remain unchanged for the present singular perturbation formulation.

The reduced-order problem of this reformulated FSP model is three-dimensional, but its solution can be obtained with a minimal computational effort, compatible for real-time implementation. The reduced-order solution is a straight-line (singular) trajectory flown by using full thrust ($\eta^r = 1$) and its direction $\chi^r = \psi_f$ can be obtained by solving two nonlinear algebraic equations. However, two integrals have to be calculated first, as

$$t - t_o = \int dt = \int_{V_o}^{V_f^r} \frac{dt}{dV} dV$$

$$= \frac{W}{g}\int_{V_o}^{V_f^r} \frac{dV}{(T_{\max} - D_0 - D_i)} \triangleq I_t(V_o V_f^r) \tag{57}$$

$$s = \int V dt = \int_{V_o}^{V_f^r} \frac{dt}{dV} V dV$$

$$= \frac{W}{g}\int_{V_o}^{V_f^r} \frac{V dV}{(T_{\max} - D_0 - D_i)} \triangleq I_s(V_o V_f^r) \tag{58}$$

Equations (57) and (58) give the time and distance needed by the interceptor to reach any velocity V_f^r starting at V_o. Based on these expressions, the interception geometry can be solved in Cartesian coordinates (see Fig. 2),

$$x(t_f) = d\cos\chi^r = R_o\cos\psi_o + V_T I_t - I_s\cos\chi^r \tag{59}$$

$$y(t_f) = d\sin\chi^r = R_o\sin\psi_o - I_s\sin\chi^r \tag{60}$$

Since I_t and I_s are functions of V_f^r only (V_o is given), Eqs. (59) and (60) can be solved by a simple one-dimensional search yielding $V_f^r(R_o,\psi_o,V_o)$ and also $\chi^r(R_o,\psi_o,V_o)$. From these results, the reduced-order adjoint variables can be also obtained as

$$\lambda_R^r = -\cos(\psi-\chi^r)/(V_f^r - V_T\cos\chi^r) \triangleq \Lambda_R^r(R,\psi,V) \tag{61}$$

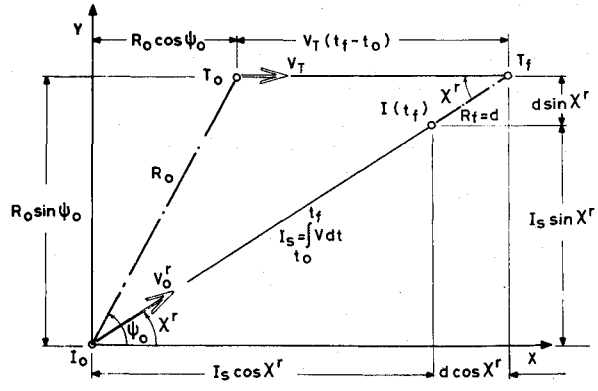

Fig. 2 Variable speed reduced-order solution.

$$\lambda_\psi^r = R\sin(\psi-\chi^r)/(V_f^r - V_T\cos\chi^r) \triangleq \Lambda_\psi^r(R,\psi,V) \quad (62)$$

$$\lambda_V^r = \frac{W}{g}\frac{V_f^r - V}{(V_f^r - V_T\cos\chi^r)(T_{\max}-D_0-D_i)} \triangleq \Lambda_V^r(R,\psi,V) \quad (63)$$

In the turning boundary layer, evaluated at a stretched time scale

$$\tau = (t-t_o)/\epsilon \quad (64)$$

one obtains, instead of Eqs. (49-56), the following set of differential equations (denoted by a superscript b):

$$\frac{dR^b}{d\tau} = \epsilon f_R(\psi^b, V^b, \chi^b), \qquad R^b(0) = R_o \quad (65)$$

$$\frac{d\psi^b}{d\tau} = \epsilon f_\psi(R^b, \psi^b, V^b, \chi^b), \qquad \psi^b(0) = \psi_o \quad (66)$$

$$\frac{dV^b}{d\tau} = \epsilon f_V(V^b, \mu^b), \qquad V^b(0) = V_o \quad (67)$$

$$\frac{d\chi^b}{d\tau} = f_\chi(V^b, \mu^b), \qquad \chi^b(0) = \chi_o \quad (68)$$

as well as

$$\frac{d\lambda_R^b}{d\tau} = -\epsilon\frac{\partial H}{\partial R^b} \quad (69)$$

$$\frac{d\lambda_\psi^b}{d\tau} = -\epsilon\frac{\partial H}{\partial \psi^b} \quad (70)$$

$$\frac{d\lambda_V^b}{d\tau} = -\epsilon\frac{\partial H}{\partial V^b} \quad (71)$$

$$\frac{d\lambda_\chi^b}{d\tau} = -\frac{\partial H}{\partial \chi^b} \quad (72)$$

In the zeroth-order approximation, with $\epsilon = 0$, all the "slow" variables (R^b, ψ^b, V^b) and the corresponding adjoints $(\lambda_R^b, \lambda_\psi^b, \lambda_V^b)$ are assumed to be frozen to their initial values at $\tau = 0$. Moreover, according to the matching principle, these values have to be equal to the initial values of the reduced-order solution.

Substituting Eqs. (51-63) into the Hamiltonian equations (22) and (27), as well as assuming an unconstrained bank angle by using Eq. (30), yields for $\tau = 0\,(t = t_o)$

$$\tan(\mu_u^b)_o = \frac{V_o}{g}\dot\chi_{ss}(V_o)\left[\frac{2V_o}{V_f^r - V_o}\right]^{1/2}\sin\left(\frac{\chi^r - \chi_o}{2}\right) \quad (73)$$

By replacing the initial conditions with the current values of the state variables, this equation leads directly to a uniformly valid feedback expression similar to Eq. (47). The only difference is that $\bar V^r$ and $\bar\chi^r$ are replaced by the improved reduced-order values of $V_f^r(R,\psi,V)$ and $\chi^r\,(R,\psi,V)$.

The accuracy of the modified zeroth-order FSP approximation [Eq. (73)] is much better than that of the previous one (47), as demonstrated by the numerical example presented in Tables 1 and 2. The geometric perturbation parameter, borrowed from the constant-speed interception[6,7], serves as a measure of the time-scale separation.

Although for this example the zeroth-order FSP accuracy is certainly adequate, for shorter initial ranges expressed by higher values of the geometrical perturbation parameter ϵ_g, further improvement may be needed. Such an improvement can be achieved by incorporaing first-order correction terms in the FSP control approximation.

Table 1 Boundary conditions and parameters for example 1

Target velocity	$V_T = 300$ m/s
Altitude	$h = 12{,}000$ m
Initial range	$R_o = 1192$ m
Initial line-of-sight angle	$\psi_o = 64.54$ deg
Initial interceptor's velocity	$V_o = 349.6$ m/s
Initial interceptor's heading	$\chi_o = -89.61$ deg
Final (capture) range d	$R_f = 2000$ m
Final angular difference $(\psi_f - \chi_f)$	$\beta_f = 0.0001$ rd
Interceptor's best turning radius at V_o	$r_{\min} = 2543.5$ m
Geometric perturbation parameter $(r_{\min}/R_o)$	$\epsilon_g = 0.2273$

Table 2 Results of example 1

Solutions	Capture time, s	Reference heading, deg	Reference velocity, m/s
Exact open-loop	$t_f^* = 105$	$\chi_f^* = 28.65$	$V_f^* = 455.2$
Previous FSP model [Eqs. (43-54)]	$\bar t_f = 111.2$	$\bar\chi^r = 41.69$	$\bar V^r = 605.2$
Modified FSP model [Eqs. (56-8)]	$\bar t_{f_0} = 105.2$	$\chi^r = 25.45$	$V_f^r = 436.8$

First-Order Forced Singular Perturbation Analysis

It can be directly verified that the only difference between the exact optimal solution given by Eqs. (27-30) and the zeroth-order FSP feedback control laws of Eqs. (47) and (73) is that in the FSP formulas the slow adjoints $(\lambda_R, \lambda_\psi, \lambda_V)$ are approximated by the zeroth-order feedback expressions of Eqs. (43-45) or (61-63), respectively. It also has to be recalled that the synthesis of the uniformly valid feedback control approximation is based on evaluating the boundary-layer control at $\tau = 0\,(t = t_o)$ as an explicit function of the initial state $(R_o, \psi_o, V_o, \chi_o)$. Since in a feedback control scheme any state along the trajectory is considered as a new initial condition, the above outlined approach leads directly to a uniformly valid explicit state-feedback control law.

It can be thus concluded that for a more accurate first-order FSP approximation the slow adjoint variables $(\lambda_R, \lambda_\psi, \lambda_V)$ have to be approximated to the first order, evaluated at $\tau = 0$, and substituted into Eqs. (27-30). The methodology of this approach is outlined in detail in a previous paper[7] dealing with a constant-speed interception. The paper also demonstrated that the first-order corrections can be expressed in an explicit feedback form. In the present paper, only the main features of this approach, based on the method of matched asymptotic expansions (MAE),[11-13] will be summarized.

The method of MAE requires that all variables of the problem be expressed by two different asymptotic expansions as a function of the perturbation parameter ϵ. One set of expansions, called the "outer" expansions (denoted by a superscript o), is expressed in the real time scale, e.g., (using R as an example),

$$R^o(t,\epsilon) = R_0^o(t) + \epsilon R_1^o(t) + \epsilon^2 R_2^o(t) + \ldots \quad (74)$$

and substituted into the original singularly perturbed differential equations such as Eqs. (49-56). The second set of expansions on the stretched time scale of Eq. (64) is called the "inner" expansions (denoted by a superscript i),

$$R^i(\tau,\epsilon) = R_0^i(\tau) + \epsilon R_1^i(\tau) + \epsilon^2 R_2^i(\tau) + \ldots \quad (75)$$

These expansions are for the boundary-layer differential equations (65-72).

According to the MAE concept, the initial conditions of the problem have to be satisfied by the "inner" expansions. The

initial values of the "outer" variables are determined by the matching condition

$$\lim_{\substack{\epsilon\to 0\\ t\to 0\\ \tau\to\infty}} [R^o(t,\epsilon)-R^i(\tau,\epsilon)]=0 \tag{76}$$

It is easy to see that the reduced-order and the boundary-layer solutions presented in the previous section are indeed the zeroth-order terms of the above expansions. Moreover, the zeroth-order matching is trivially satisfied for all the slow variables, because they remain constant in the boundary layer.

The matching of first-order terms is more complicated. The first-order boundary layer equation (for R, for example) is

$$\frac{dR_1^i(\tau)}{d\tau}=f_R[\psi_0^i(\tau),V_0^i(\tau),\chi_0^i(\tau)],\quad R_1^i(0)=0 \tag{77}$$

Since $\psi_0^i(\tau)=\psi_0, V_0^i(\tau)=V_o$ and $\chi_0^i(\tau)$ is obtained, by integrating Eq. (68) and using Eq. (73), as

$$\chi_0^i(\tau)=\chi_o+\int_0^\tau f_\chi[V_o,\mu_0^i(V_o,\chi_0^i)]\,d\tau \tag{78}$$

$R_1^i(\tau)$ can be computed by a direct quadrature

$$R_1^i(\tau)=\int_0^\tau f_R[\psi_o,V_o,\chi_0^i(\tau)]\,d\tau \tag{79}$$

Based on this feature, the first-order matching condition, which determines the initial value of R_1^0, is

$$R_1^o(t_o)=\lim_{\tau\to\infty}\int_0^\tau\{f_R[\psi_o,V_o,\chi_0^i(\tau)]-f_R[\psi_o,V_o,\chi_0^o]\}d\tau \tag{80}$$

where (of course)

$$\chi_0^o=\chi_0^o(R_o,\psi_o,V_o)=\chi^r(R_o,\psi_o,V_o) \tag{81}$$

Similar equations can be written for the other slow variables as well. These quadratures can be carried out either as a function of τ along the zeroth-order trajectory (which is an open-loop process) or can be expressed in a feedback form by replacing τ as the independent variable of the integration with the zeroth-order fast variable χ_0^i. Since from Eq. (68)

$$d\chi_0^i=f_\chi[V_o,\mu_0^i(V_o,\chi^r,\chi_0^i)]\,d\tau \tag{82}$$

Eq. (80) can be rewritten as

$$R_1^o(t_o)\triangleq I_R=\int_{\chi_o}^{\chi^r}\frac{[f_R(\psi_o,V_o,\chi_0^i)-f_R(\psi_o,V_o,\chi_o^r)]}{f_\chi(V_o,\chi^r,\chi_0^i)}d\chi_0^i \tag{83}$$

Fortunately, Eq. (83) can be solved in a closed form

$$I_R=\frac{4[2V_o(V_f-V_o)]^{1/2}}{\dot\chi_{ss}(V_o)}\sin[(\psi_o-\chi^r)+\frac{\chi^r-\chi_0^i}{4}]\cdot\sin\left(\frac{\chi^r-\chi_0^i}{4}\right) \tag{84}$$

By similar steps, the initial values of the other first-order state variables can also be computed

$$\psi_1^o(t_o)\triangleq I_\psi=\frac{4[2V_o(V_f-V_o)]^{1/2}}{R_0\dot\chi_{ss}(V_o)}\cos\left[(\psi_o-\chi^r)+\frac{\chi^r-\chi_0^i}{4}\right]\cdot\sin\left(\frac{\chi^r-\chi_0^i}{4}\right) \tag{85}$$

$$V_1^o(t_o)\triangleq I_V=-\frac{4V_o^2D_i\dot\chi_{ss}(V_o)}{gW}\left(\frac{2V_o}{V_f-V_o}\right)^{1/2}\sin^2\left(\frac{\chi^r-\chi_0^i)}{4}\right) \tag{86}$$

The integrals I_R, I_ψ, I_V represent the differences between the variations of the respective slow variables in the zeroth-order turning boundary layer and in the reduced-order solution. If the initial conditions are such that $\chi_o=\chi^r(R_o,\psi_o,V_o)$ (i.e., no turning is required), all of these correction terms vanish.

With the initial values of Eqs. (84–86) in hand, the first-order outer solution can be evaluated. The most convenient way is to use the two first terms of the expansions jointly, by defining

$$R_{0-1}^o(t)\triangleq R_0^o(t)+\epsilon R_1^o(t) \tag{87}$$

and doing the same for the other variables. (Note that for the presently used FSP model $\epsilon=1$.)

Substituting the respective sum terms in Eq. (52) yields to first-order

$$\mu_{0-1}^o(t)=0 \tag{88}$$

i.e., that the solution of the "outer" problem, corrected by first-order terms, is (similarly to the reduced-order solution) also a straight-line trajectory.

Therefore, the solutions can be directly obtained by replacing in Eqs. (57–63) the initial conditions (R_o,ψ_o,V_o) by $(R_o+\epsilon I_R,\psi_o+\epsilon I_\psi,V_o+\epsilon I_V)$. This process yields

$$\chi_{0-1}^o=\chi^r(R_{0-1}^o,\psi_{0-1}^o,V_{0-1}^o) \tag{89}$$

$$V_{f_{0-1}}^o=V_f(R_{0-1}^o,\psi_{0-1}^o,V_{0-1}^o) \tag{90}$$

and consequently also

$$\lambda_{R_{0-1}}^o=\Lambda_R^r(R_{0-1}^o,\psi_{0-1}^o,V_{0-1}^o) \tag{91}$$

$$\lambda_{\psi_{0-1}}^o=\Lambda_\psi^r(R_{0-1}^o,\psi_{0-1}^o,V_{0-1}^o) \tag{92}$$

$$\lambda_{V_{0-1}}^o=\Lambda_V^r(R_{0-1}^o,\psi_{0-1}^o,V_{0-1}^o) \tag{93}$$

The next step is to compute the slow adjoint variables of the first-order "inner" solution. In Eq. (69), the first-order terms give

$$\frac{d\lambda_{R_1}^i}{d\tau}=-\frac{\partial H_0^i}{\partial R_0^i}=-\left(\lambda_{R_0}^i\frac{\partial f_R^i}{\partial R_0^i}+\lambda_{\psi_0}^i\frac{\partial f_\psi^i}{\partial R_0^i}\right) \tag{94}$$

This differential equation, as well as the similar ones for $\lambda_{\psi_1}^i$ and $\lambda_{V_1}^i$, can be solved by direct quadrature, since the right-hand side contains only zeroth-order terms known from earlier steps,

$$\lambda_{R_1}^i(\tau)=\lambda_{R_1}^i(0)-\int_0^\tau\left(\frac{\partial H_0^i}{\partial R_0^i}\right)d\tau \tag{95}$$

The initial value $\lambda_{R_1}^i(0)$ is, however, unknown. It has to be obtained by applying the appropriate matching condition, which is expressed by[13]

$$\lambda_{R_1}^i(0)=\lambda_{R_1}^o(t_o)+\epsilon I_{\lambda_R} \tag{96}$$

where

$$I_{\lambda_R}\triangleq\lim_{\tau\to\infty}\int_0^\tau\left[\frac{\partial H_0^i}{\partial R_0^i}(\tau)-\frac{\partial H_0^o}{\partial R_0^o}(t_o)\right]d\tau \tag{97}$$

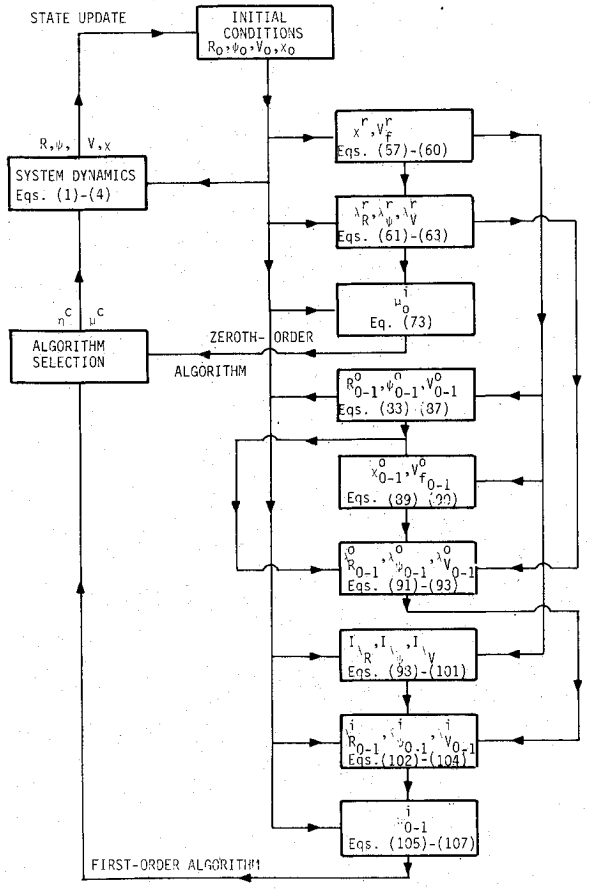

Fig. 3 Flowchart of the FSP feedback control implementation.

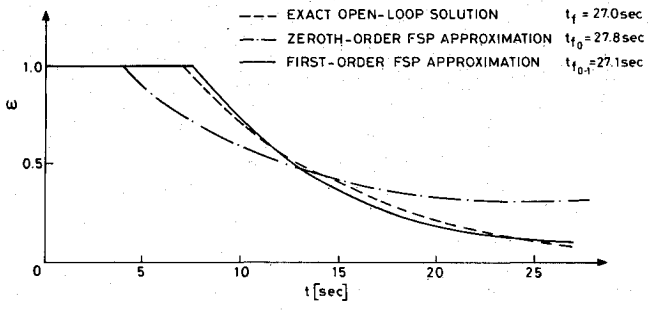

Fig. 4 Normalized bank angle history (example 2).

Expressions similar to Eqs. (96) and (97) are valid for $\lambda^i_{\psi_1}(0)$ and $\lambda^i_{V_1}(0)$ as well. By using Eq. (82), the integrals I_{λ_R}, I_{λ_ψ}, and I_{λ_V} can be obtained in a closed form. Inspection of Eqs. (97), (23), (24), and (61-62) reveals that

$$I_{\lambda_R} = -\Lambda^r_\psi(R_o,\psi_o,V_o)I_\psi/R_o \tag{98}$$

$$I_{\lambda_\psi} = \Lambda^r_R(R_o,\psi_o,V_o)R_oI_\psi - \Lambda^r_\psi(R_o,\psi_o,V_o)I_R/R_o \tag{99}$$

while I_{λ_V} is obtained independently from

$$I_{\lambda_V} \triangleq \int_{\chi_o}^{\chi^r}\left[\frac{\partial H^i_0}{\partial V^i_0} - \frac{\partial H^o_0}{\partial V^o_0}\right]\frac{\mathrm{d}\chi^i_0}{f_\chi(V_o,\chi^r,\chi^i_0)} \tag{100}$$

$$I_{\lambda_V} = -\frac{-4(1+V_o/K(\mathrm{d}K/\mathrm{d}V)\,|V_o)}{(V^r_f - V_T\cos\chi^r)\dot{\chi}_{ss}(V_o)} \times\left[\frac{2(V^r_f-V_o)}{V_o}\right]^{1/2}\cdot\sin^2\left(\frac{\chi^r-\chi^i_0}{4}\right) \tag{101}$$

Table 3 Boundary conditions and parameters for example 2

Target velocity	$V_T = 350$ m/s
Altitude	$h = 12{,}000$ m
Initial range	$R_o = 6318.48$ m
Initial line-of-sight angle	$\psi_o = 18.87$ deg
Initial interceptor's velocity	$V_o = 598.17$
Initial interceptor's heading	$\chi_o = -44.39$ deg
Final (capture) range d	$R_f = 2000$
Final angular difference $(\psi_f - \chi_f)$	$\beta_f = 0.025$ rd
Interceptor's best turning radius at $V = V_o$	$r_{\min} = 7447.10$ m
Geometric perturbation parameter $(r_{\min}/R_o)$	$\epsilon_g = 1.1786$

Table 4 Results of example 1

Solution	Capture time, s	Reference heading, deg	Reference velocity, m/s
Exact open-loop	$t^*_f = 27.0$	$\chi^*_f = 28.65$	$V^*_f = 543.4$
Zeroth-order FSP [Eqs. (49-73)]	$t_{f_0} = 27.8$	$\chi^r = 9.6$	$V^r_f = 600.1$
First-order FSP model [Eqs. (83-107)]	$t_{f_{0-1}} = 27.1$	$\chi^o_{0-1} = 26.2$	$V^o_{f_{0-1}} = 555.4$

Based on Eqs. (98-101), the initial values of the slow adjoint variables in the inner solution can be corrected to the first-order,

$$\lambda^i_{R_{0-1}}(0) = \Lambda^r_R(R^o_{0-1},\psi^o_{0-1},V^o_{0-1}) + \epsilon I_{\lambda_R}(R_o,\psi_o,V_o,\chi_o) \tag{102}$$

and similarly

$$\lambda^i_{\psi_{0-1}}(0) = \Lambda^r(R^o_{0-1},\psi^o_{0-1},V^o_{0-1}) + \epsilon I_{\lambda_\psi}(R_o,\psi_o,V_o,\chi_o) \tag{103}$$

$$\lambda^i_{V_{0-1}}(0) = \Lambda^r_V(R^o_{0-1},\psi^o_{0-1},V^o_{0-1}) + \epsilon I\Lambda_V(R_o,\psi_o,V_o,\chi_o) \tag{104}$$

Substituting Eqs. (102-104) into the Hamiltonian [Eq. (22)] and applying the necessary conditions of optimality [Eqs. (27) and (30)] one obtains the following expression for the optimal bank angle:

$$\mu^i_{0-1}(0) = \mathrm{sat}[\tan^{-1}\phi(R_o,\psi_o,V_o,\chi_o)] \tag{105}$$

where

$$\phi^2(R_o,\psi_o,V_o,\chi_o) = \frac{W}{gD_i(V_o)}\left[\frac{1-\lambda^i_{R_{0-1}}f_R - \lambda^i_{\psi_{0-1}}f_\psi}{\lambda^i_{V_{0-1}}} - f_V(V_o,0)\right] \tag{106}$$

and the sign is determined by

$$\mathrm{sign}[\mu^i_{0-1}(0)] = \mathrm{sign}[\chi^o_{0-1}(R_o,\psi_o,V_o,\chi_o) - \chi_o] \tag{107}$$

Since all terms in Eqs. (105-107) depend explicitly on the initial state, the synthesis of a uniformly valid feedback control law directly follows. The flowchart of this feedback control implementation is shown in Fig. 3.

In order to evaluate the accuracy of this new feedback control approximation, an example of a very short-range interception was selected.

The initial conditions for this numerical example and the results of the comparison to the exact solution are presented in Tables 3 and 4. In Fig. 4, the time histories of the normalized bank angle, defined as

$$\omega \triangleq \mu/\mu_{\max} \tag{108}$$

are depicted for each case ($n_{max} = 5$) with

$$\mu_{max} = \cos^{-1}[1/5] = 78.5 \text{ deg} \quad (109)$$

The results show that the payoff error of the zeroth-order approximation is of the order of 3%. The error in the reference (predicted final) values is even larger. The first-order FSP solution is rather successful in predicting the final values of the state variables and, as a consequence, it provides an outstanding payoff accuracy even for an engagement starting within the best turning circle of the interceptor.

The improved accuracy comes at the expense of some additional computations. Although in relative terms the first-order algorithm requires about twice as much CPU time as the modified zeroth-order version and about 2.8 times more than the previous FSP model, in absolute terms, the overall computational effort is very modest. Most computational steps are of an algebraic nature. This effort, characterized by a computational speed of 1/100 of real time on an IBM 370/168, is certainly well within the range of real-time airborne implementation.

Conclusions

In the present paper, an improved forced singular perturbation algorithm was presented for the synthesis of a uniformly valid feedback control law of a minimum-time air-to-air interception in the horizontal plane. The improvements correct the effects of imperfect time scale separation of previous algorithms by including the velocity dynamics in the reduced-order problem and by incorporating first-order correction terms in the control law.

The accuracy obtained by the improved algorithm is very impressive, as demonstrated by numerical examples for a realistic aircraft model. The new algorithm allows the extension of the domain of practical validity of the forced singular perturation feedback approximation (guaranteeing payoff errors less than 1%) down to initial ranges of the order of the interceptor's best turning radius. The additional computational effort required to incorporate the improvements is very modest and does not adversely affect the potential for real-time on-line implementation of the feedback control approximation. The good accuracy in an enlarged domain of operation provides an improved building block for an automated guidance algorithm for minimum-time air-to-air interception.

Acknowledgment

This work was performed when the first author was a Visiting Senior Research Assistant with the Dept. of Aeronautical Engineering, Technion—Israel Institute of Technology. The work was supported in part by the Technion VPR—Seniel Ostrow Research Fund under Grant 161-462.

References

[1]Shinar, J. and Merari, A., "Aircraft Performance Optimization by Forced Singular Perturbation," *Proceedings of 12th Congress of ICAS,* 1980, pp. 758-772.

[2]Shinar, J., Negrin, M., Well, K.H., and Berger, E., "Comparison Between the Exact Approximate Feedback Solutions for Medium Range Interception Problems," Paper presented at Joint Automatic Control Conference, Charlottesville, VA, 1981.

[3]Negrin, M. and Shinar, J., "Solution of Three-Dimensional Interception by Inclined Plane Using the Forced Singular Perturbation Technique," Paper presented at 24th Israel Annual Conference on Aviation and Astronautics, Haifa, Israel, 1982.

[4]Calise, A.J., "A Singular Perturbation Analysis of Optimal Aerodynamic and Thrust Magnitude Control," *IEEE Transactions on Automatic Control,* Vol. AC-24, No. 5, 1979, pp. 720-729.

[5]Shinar, J., "On Applications of Singular Perturbation Techniques in Nonlinear Optimal Control," *Automatica,* Vol. 19, No. 2, 1983, pp. 203-211.

[6]Breakwell, J.V., Shinra, J., and Visser, H.G., "Uniformly Valid Feedback Expansions for Optimal Control of Singularly Perturbed Dynamic Systems," *Journal of Optimization, Theory and Applications,* Vol. 46, No. 4, 1985, pp. 441-454.

[7]Visser, H.G. and Shinar, J., "First-Order Corrections in Optimal Feedback Control of Singularly Perturbed Nonlinear Systems," *IEEE Transactions on Automatic Control,* Vol. AC-31, No. 4, May 1986.

[8]Simakova, E.N.,"The Quality Problem in Pursuit Games for Inertial Systems," *Automation and Remote Control,* April 1975, pp. 1716-1724.

[9]Calise, A.J., "Singular Perturbation Methods for Variational Problems in Aircraft Flight," *IEEE Transactions on Automatic Control,* Vol. AC-21, No. 3, 1976, pp. 345-353.

[10]Mehra, R.K. et al., "A Study of the Application of Singular Perturbation Theory," NASA CR 3167, 1979.

[11]Wasow, W., *Asymptotic Expansions for Ordinary Differential Equations,* Interscience, New York, 1965.

[12]Freedman, M.I. and Granoff, B., "Formal Asymptotic Solutions of a Singularly Perturbed Nonlinear Optimal Control Problem," *Journal of Optimization, Theory and Applications,* Vol. 19, 1976, pp. 301-325.

[13]Ardema, M.D., "An Introduction to Singular Perturbations in Nonlinear Optimal Control," *Singular Perturbations in Systems and Control,* edited by M.D. Ardema, Springer Verlag, Vienna, 1982, pp. 1-92.